



Fermi National Accelerator Laboratory

FERMILAB-Conf-98/356-E

D0

The Silicon Microstrip Tracker for the D0 Upgrade

Maria Teresa P. Roco
For the D0 Collaboration

*Fermi National Accelerator Laboratory
P.O. Box 500, Batavia, Illinois 60510*

December 1998

Will be Published in *Nuclear Physics B Proceedings Supplement*
Published Proceedings of the *6th International Conference on Advanced Technology and Particle Physics*, Como, Italy, October 5-9, 1998

Disclaimer

This report was prepared as an account of work sponsored by an agency of the United States Government. Neither the United States Government nor any agency thereof, nor any of their employees, makes any warranty, expressed or implied, or assumes any legal liability or responsibility for the accuracy, completeness, or usefulness of any information, apparatus, product, or process disclosed, or represents that its use would not infringe privately owned rights. Reference herein to any specific commercial product, process, or service by trade name, trademark, manufacturer, or otherwise, does not necessarily constitute or imply its endorsement, recommendation, or favoring by the United States Government or any agency thereof. The views and opinions of authors expressed herein do not necessarily state or reflect those of the United States Government or any agency thereof.

Distribution

Approved for public release; further dissemination unlimited.

Copyright Notification

This manuscript has been authored by Universities Research Association, Inc. under contract No. DE-AC02-76CHO3000 with the U.S. Department of Energy. The United States Government and the publisher, by accepting the article for publication, acknowledges that the United States Government retains a nonexclusive, paid-up, irrevocable, worldwide license to publish or reproduce the published form of this manuscript, or allow others to do so, for United States Government Purposes.

The Silicon Microstrip Tracker for the DØ Upgrade

M. Roco^a

For the DØ Collaboration

^aFermi National Accelerator Laboratory
MS 357 P.O. Box 500
Batavia, IL. 60510-0500 U.S.A

The silicon microstrip tracker is a major element of the DØ detector upgrade at Fermilab. After a general overview of the silicon tracker design, results are presented for a series of detector and electronics performance studies which include beam tests and proton irradiation. Charge sharing and strip-to-strip uniformity studies using an infrared laser are also presented.

1. INTRODUCTION

The Fermilab Tevatron luminosity upgrade program involves the replacement of the existing Main Ring accelerator with the Main Injector and the construction of a new antiproton storage ring within a common tunnel. The ultimate goal is to accumulate between 2-5 fb⁻¹ of data, with typical luminosities of $\sim 0.5\text{-}2 \times 10^{32} \text{ cm}^{-2}\text{s}^{-1}$. The center-of-mass energy will increase to 2 TeV and the bunch crossing interval will be reduced from 3.5 μs to 396 ns, and eventually to 132 ns. Detector upgrades for both collider experiments [1], DØ and CDF, are presently underway to cope with the higher event rates and backgrounds, and to optimize their physics capabilities in the new high luminosity Main Injector era.

2. DØ TRACKING SYSTEM UPGRADE

A major element of the DØ detector upgrade involves the replacement of the inner tracking system. The momenta of charged particles are determined from their curvature in a 2 Tesla axial magnetic field provided by a 2.8 m long superconducting solenoid consisting of a two layer coil with a mean radius of 60 cm. An annular preshower detector is installed in the small gap between the solenoid coil and the central calorimeter cryostat. It is designed to enhance the identification of electrons and photons, measure their precise position in the region $|\eta| < 1.2$, and compensate

for the energy losses in the solenoid.¹ The central preshower consists of three layers of 7 mm base triangular scintillating strips with wavelength-shifting fiber readout. Fast energy and position measurements enable the use of the preshower information at the trigger level. Simulation studies show that the central preshower information allows the electron trigger rate to be reduced by a factor of 3-5 without a loss in efficiency. There are also forward preshower detectors mounted on the face of each end calorimeter cryostat. Like the central preshower detector, they are intended to improve the electron identification and triggering capabilities by making precise position measurements of particle trajectories using dE/dx and showering information.

The solenoid encloses the scintillating fiber tracker and the silicon microstrip tracker. The fiber tracker provides charged particle track reconstruction and momentum measurement within $|\eta| < 2$, and fast level 1 track triggering. It consists of eight concentric barrels of scintillating fiber doublet layers. It has an active length of 2.6 m and a radial coverage of 20 cm $< r < 50$ cm. There are approximately 77,000 fibers connected to photodetectors via 11 m long clear waveguides. The optical signals from the fibers are detected by visible light photon counters (VLPC), which are arsenic-doped silicon diodes with operating

¹The superconducting coil, together with the cryostat, corresponds to about 1.1 radiation lengths of material.

temperatures typically between 8-10 K. A large sample of VLPCs were tested in a cosmic ray test stand [2]. The VLPC sample exhibited $\sim 80\%$ quantum efficiency, relatively high gain and less than 0.1% average noise occupancy when operated at full efficiency. The doublet hit efficiency for cosmic ray tracks is better than 99.9% and a position resolution $\sim 100 \mu\text{m}$ is obtained. The region $r < 18 \text{ cm}$ is occupied by the $\sim 800,000$ channel silicon microstrip tracker [3] (SMT), its support structure, cooling manifolds, and cabling. The SMT is designed to provide critical tracking information for pattern recognition, achieve optimum resolution for momentum and vertex reconstruction over the full pseudorapidity coverage of $D\phi$, and provide the capability to identify displaced secondary vertices from short-lived particle decays.

3. OVERVIEW OF THE SMT DESIGN

The main factors which drive the design of the silicon microstrip tracker include: the long luminous region, performance requirements which include three-dimensional track reconstruction capabilities with z -vertex and transverse impact parameter resolutions better than $30 \mu\text{m}$, radiation hardness to cope with the expected Run 2 delivered luminosity, and electronics and readout which can operate reliably with bunch crossing intervals down to 132 ns.

The extended interaction region ($\sigma_Z = 25 \text{ cm}$) sets the length scale and motivates a design which consists of disk and barrel modules shown in Fig. 1. There are six disk/barrel modules supported by a double-walled carbon-fiber/epoxy half-cylinder which aids in maintaining the precise relative alignment and supports the detector cabling and cooling services. Each barrel, 12.4 cm in length, contains four concentric layers (1-4) of silicon ladders with radii ranging from 2.6 cm to 10 cm. The ladder, which is the basic detector unit, consists of two $300 \mu\text{m}$ thick wafers, $6 \text{ cm} \times 2.1 \text{ cm}$, positioned end to end and electrically connected by micro-wirebonds. The wafers are held in position by two longitudinal rails consisting of a carbon fiber composite and Rohacell foam sandwich. Layers 2 and 4 are double-sided

with $50 \mu\text{m}$ pitch strips on the p -side while the n -side has $62.5 \mu\text{m}$ pitch strips at 2° stereo angle relative to the beam axis. The four inner barrels include 90° stereo double-sided detectors in layers 1 and 3, with $50 \mu\text{m}$ and $156 \mu\text{m}$ pitch strips on the p and n -side, respectively. The outer barrels have $50 \mu\text{m}$ pitch single-sided ladders in layers 1 and 3.

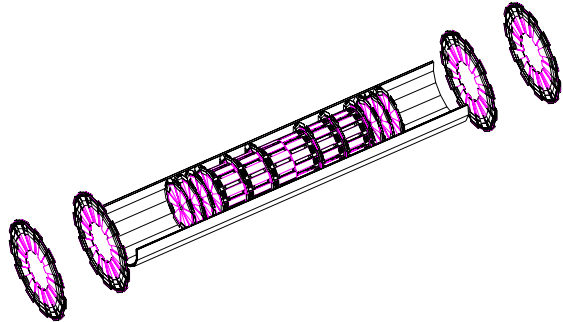


Figure 1. *The silicon microstrip tracker consists of disks interspersed with barrels.*

The ladders, as well as the fiber tracker VLPC system, are read out by radiation hard CMOS custom integrated circuits, SVX-IIe chips [4], which were optimized for 396 ns and 132 ns bunch crossing intervals. The SVX-IIe chip, with an average power dissipation of 0.64 W, is a 128 channel device which consists of preamplifiers, 32 cell deep analog pipelines, 8 bit ADCs, and sparsification². The highly flexible SVX-IIe chip has programmable test pulse patterns, ADC ramp, pedestal, bandwidth and polarity. It has been designed to read out on each edge of a 53 MHz clock and is operational beyond 70 MHz. The SVX-IIe chips and associated readout electronics are mounted on a flexible kapton circuit (HDI). During the ladder construction, the HDI is glued to a $300 \mu\text{m}$ thick beryllium substrate. The substrate provides a thermal path from the readout heat sources to the coolant channels, maintains the flatness of the HDI and includes precisely machined notches for ladder positioning

²This allows the readout only of those channels, and their nearest neighbors, above a certain specified threshold.

and stability. The readout electronics and their supports are mounted inboard on the active surface of the silicon to minimize the uninstrumented gaps between inter-barrel/disk modules.

The ladders are mounted on beryllium bulkheads which have tight tolerances since they establish the precision of the alignment. By means of an integrated coolant channel, active bulkheads also provide the necessary cooling for the electrical components mounted at one end of the ladders. The coolant consists of a mixture of deionized ethylene glycol and water, and has a freezing point of $-10\text{ }^{\circ}\text{C}$. Radiation damage effects lead to an increase in the detector leakage current. To cope with the high radiation environment expected in Run II the detectors are operated at temperatures between $5\text{-}10\text{ }^{\circ}\text{C}$.

The disks in the central and forward regions provide three-dimensional track reconstruction and improve the tracking at large η . Disks interspersed with the barrels consists of 12 overlapping wedges with an active area $2.5\text{ cm} < r < 9.8\text{ cm}$. Larger radii disks with $9.6\text{ cm} < r < 23.6\text{ cm}$ at $z = \pm 94\text{ cm}$ and $\pm 126\text{ cm}$, provide improved momentum resolution up to $|\eta| = 3$. The central disks have double-sided wedge detectors with $\pm 15^{\circ}$ stereo and forward disks have single-sided wedge detectors, glued back to back, with an effective $\pm 7.5^{\circ}$ stereo. The wedges in the central and the forward disks are mounted around a thin beryllium cooling pipe.

4. BEAM TESTS RESULTS

Extensive tests of a number of silicon detectors and the final version of the SVX-IIe chip and readout electronics were performed at a Fermilab test beam facility equipped with a 2 Tesla magnet. A description of the test devices, readout electronics, test beam setup and analysis can be found in refs [5] [6].

The cluster charge for normally incident particles for the single-sided test ladder, operated at room temperature with $B = 0$, is shown in Fig. 2. The signal to noise ratio S/N is defined as Q_{mp}/σ_N , where Q_{mp} is the most probable value of the cluster charge. To obtain Q_{mp} the distribution in Fig. 2 is fitted with a Gaussian convoluted

Landau distribution as shown. Since the channel-to-channel variation of the random noise for the same SVX-II chip is small, the average, σ_N , is used in the analysis. A signal to noise ratio of 21 is obtained for the single-sided test ladder, with a mean equivalent noise charge of $\sim 1200\text{ }e^-$.

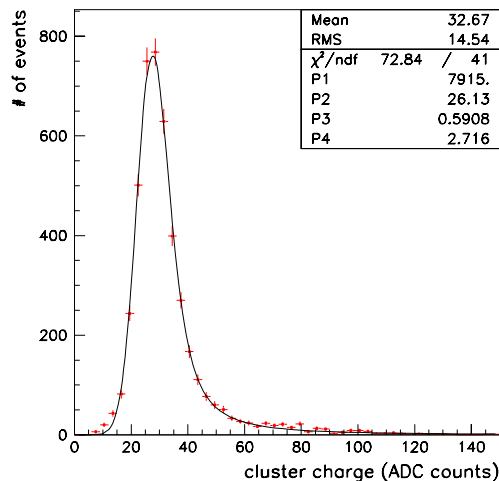


Figure 2. The cluster charge distribution for the ladder fitted with a Gaussian convoluted Landau function gives a most probable value of 26 ADC counts (equivalent to $\sim 25,000\text{ }e^-$) for 1 mip.

The charge cluster profile is obtained by fitting a track through the telescope elements. Fig.3 shows the width of the charge cluster profiles in the single-sided ladder for 125 GeV pions at normal incidence, and for data where the ladder is rotated with $\phi = 15^{\circ}$ and 30° about an axis through the center of the detector parallel to the strips. As expected, these plots show charge profiles which are symmetric around the hit position, with increasing widths for inclined tracks, extending up to four strips at $\phi = 30^{\circ}$.

The residuals for tracks at normal incidence, plotted in Fig.4, include measurement errors from the intrinsic resolutions of the telescope elements used in the track fit, as well as systematic uncertainties associated with multiple scattering. After correcting for these contributions, a spatial resolution better than $9\text{ }\mu\text{m}$ is obtained.

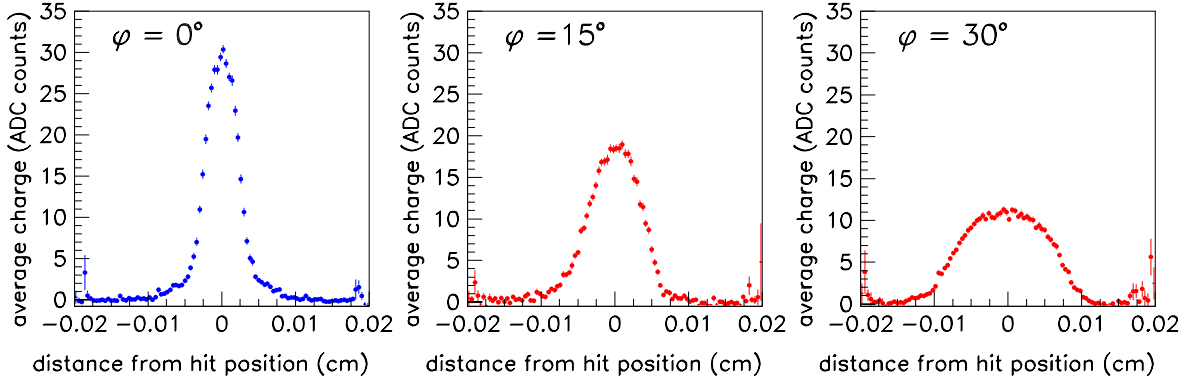


Figure 3. Charge cluster profiles using tracks for values of ϕ at 0° , 15° and 30° ($B = 0$). The vertical axis shows the average charge in ADC counts and the horizontal axis gives the distance from the track hit position in cm.

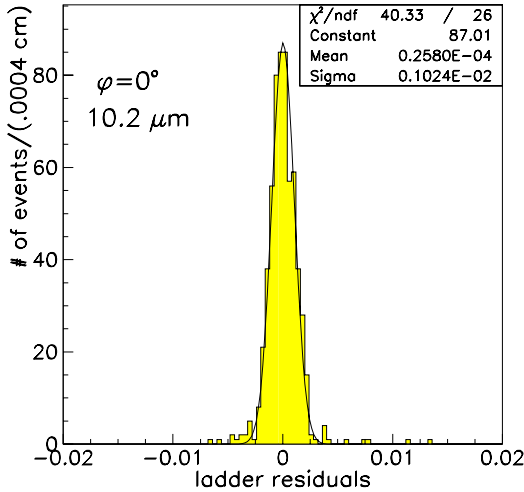


Figure 4. Track residuals in the single-sided test ladder ($B = 0$) for normally incident pions.

5. IRRADIATION TESTS

A major issue relevant to the long-term operation of silicon detectors is their tolerance to large particle fluences. The expected radiation dose for the innermost layer of the DØ silicon tracker is 0.5 MRad/fb^{-1} . To study the extent of radiation damage at 2 fb^{-1} , a few test detec-

tors, some instrumented with SVX-II chips, were irradiated with an 8 GeV proton beam from the Fermilab booster accelerator. The effects of the radiation damage were manifested by an increase in the detector leakage current and full depletion voltage. The behavior of the detector leakage current with increasing radiation dose is shown in Fig.5 as a function of the bias voltage for a double-sided detector.

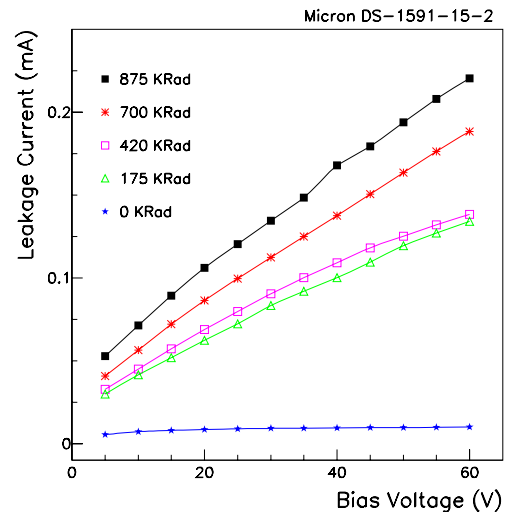


Figure 5. Leakage current as a function of V_{bias} for increasing values of radiation dose.

After irradiation, a significant increase in the noise, attributed to an increase in the detector leakage current, was reported in [6]. Recent measurements for a double-sided detector gave similar results; assuming no degradation in the charge collection efficiency, the signal to noise ratio, after a dose of 1 MRad, decreases by about 30% and 40% in the n and p side, respectively. It should be noted that these measurements and those previously reported in [6] were performed at room temperature. Detector leakage currents are temperature dependent [7] and can be significantly reduced by operating the detectors at lower temperatures.

Radiation induced changes in the doping concentration affect the value of the depletion voltage which can reach very high values after years of operation in a high radiation environment. The external bias will eventually fail to fully deplete the detector, or would have to be chosen so high that excessive breakdown currents would prevent reliable operation. These studies show that after a dose of 1 MRad, a single-sided ladder, which initially depleted at 35 V, was functional beyond a bias voltage of 200 V and did not exhibit any sign of breakdown.

6. LASER TEST STAND RESULTS

Measurements before and after irradiation were performed using a laser test stand setup with a 1064 nm infrared laser. The focusing system consists of a collimating lens and an adjustable post holder which allows vertical positioning of the lens relative to the test detector. The height of the lens and the laser beam attenuation were adjusted to give a narrow beam with a Gaussian width of $\sim 10\mu\text{m}$.

The dependence of the cluster width on the bias voltage is shown in Fig.6, before and after the irradiation. Before irradiation, the cluster width on the p -side is always narrow, independent of the bias voltage. The n -side cluster width decreases with increasing bias voltage and plateaus after the full depletion voltage is reached. The effect of radiation damage is to create p -type centers in the bulk silicon. Changes in the doping concentration cause type inversion of the silicon from n -type

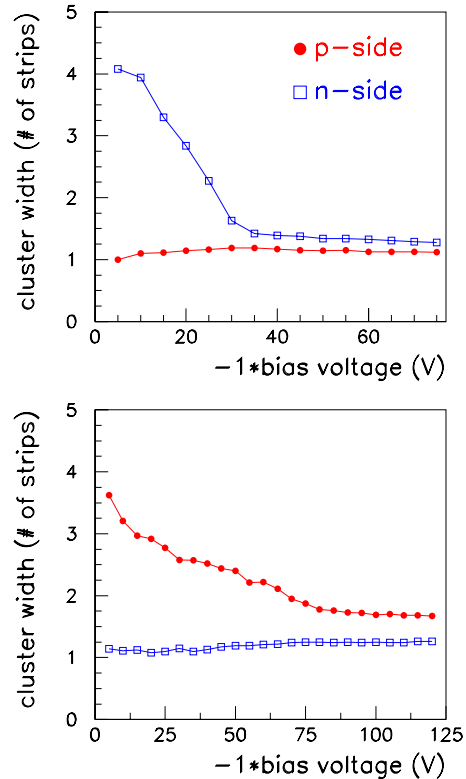


Figure 6. Cluster width versus the bias voltage for the p -side (dots) and n -side (squares) before (top) and after 1 MRad irradiation (bottom).

to p -type. The bottom plot of Fig.6 shows the behavior of the cluster width after type inversion has occurred.

A fine scan of a single-sided ladder was also performed to study charge sharing and the strip-to-strip uniformity of the response. Data taking was performed while moving the laser beam across the detector strips at fine intervals of $\sim 2.5\mu\text{m}$. The charge asymmetry η is shown in Fig.7 as a function of the beam position for two consecutive strips L and R . The parameter η is defined as $\eta = (Q_L - Q_R)/(Q_L + Q_R)$, where Q_L and Q_R are the pedestal corrected pulse heights in strips L and R , respectively. The parameterized result from the test beam is shown for comparison and is found to be in good agreement with the laser scan data.

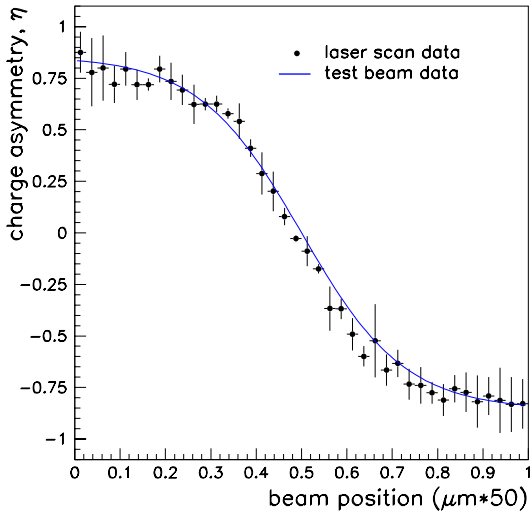


Figure 7. The charge asymmetry parameter, $\eta = (Q_L - Q_R)/(Q_L + Q_R)$, for two consecutive strips, is plotted as a function of the laser beam position and compared to the parameterized test beam result shown as the curve.

The strip-to-strip uniformity of the response across the single-sided ladder is shown in Fig. 8. These results show that about 85% of the channels are within the $\pm 2\%$ range shown. Over 95% of the channels are within a $\pm 3\%$ range.

7. SUMMARY

The construction of the DØ silicon microstrip tracker is currently underway. The performance of a number of production silicon microstrip detectors and the readout electronics has been extensively studied. Results of measurements from the test beam, irradiation, and laser test stand have been presented. These studies have been very useful in terms of characterizing the electrical properties of the silicon detectors, and understanding the critical operational parameters of the SVX-IIe chip and the readout electronics to ensure their optimal operation given the Run II Tevatron running conditions.

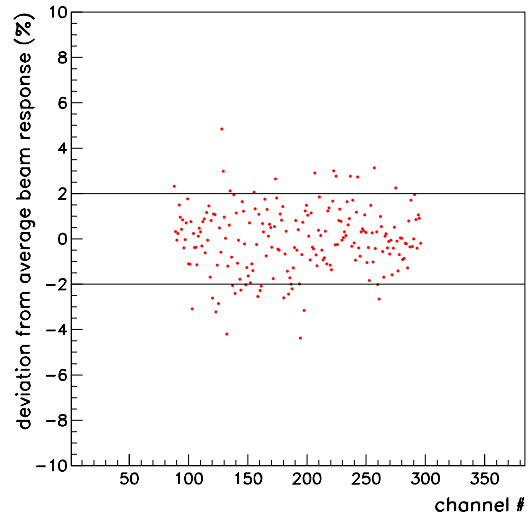


Figure 8. Channel-to-channel uniformity. The deviation from the average beam response for the scanned channels in the single-sided ladder versus the channel number. 15% of the channels are outside the $\pm 2\%$ range shown and 4% are outside $\pm 3\%$ range.

REFERENCES

1. DØ Collab.,FERMILAB-PUB-96-357(1996)
CDF Collab.,FERMILAB-PUB-96-390(1996)
2. D. Adams et. al., IEEE Trans. Nucl. Sci. 43 (1996) 1146.
3. DØ Collab., The DØ Silicon Tracker Technical Design Report, Fermilab (1995).
4. R. Yarema et.al., FERMILAB-TM-1892 (1994).
5. R. Lipton for the DØ Collab., Nucl. Inst. and Meth. A 418(1998).
6. M. Roco for the DØ Collab., Nucl. Inst. and Meth. A 418(1998).
7. E. Barberis et. al., Nucl. Inst. Meth. A 326(1993) 373.
8. E. Belau et. al., Nucl. Inst. and Meth. A 214 (1983) 253.